

All-optical coherently controlled terahertz ac charge currents from excitons in semiconductors

Christian Sames,¹ Jean-Michel Ménard,¹ Markus Betz,¹ Arthur L. Smirl,² and Henry M. van Driel^{1,*}

¹*Department of Physics and Institute for Optical Sciences, University of Toronto, Toronto, Ontario, Canada M5S 1A7*

²*Laboratory for Photonics and Quantum Electronics, 138 IATL, University of Iowa, Iowa City, Iowa 52242, USA*

(Received 22 September 2008; revised manuscript received 11 December 2008; published 22 January 2009)

We have investigated the influence of excitonic effects on two-color coherently controlled electrical currents in semiconductors. We produce currents in CdSe and CdTe at temperature of 10 or 80 K using quantum interference between single- and two-photon absorption of fundamental and second-harmonic 150 fs optical pulses tuned over a wide energy range. Current injection is monitored via the emitted terahertz generation. For the highest photon energies wherein the injected electron-hole kinetic energy is large compared to the exciton binding energy, “dc” electrical current injection is observed and expected within the independent-particle approximation in which phase control of the current magnitude is governed by the optical phases only. However, as the photon energy decreases to the band-gap energy, features appear in the terahertz emission pattern that increasingly signal the breakdown of this model, in agreement with recent theoretical calculations that incorporate electron-hole interactions. In particular, when the excitation pulse bandwidth spans the $1s$ - $2p$ exciton states, the terahertz emission characteristics are consistent with a theoretically predicted ac electrical current injection in which the phase of the current—but not its amplitude—is controlled by the relative phase of the optical pulses.

DOI: [10.1103/PhysRevB.79.045208](https://doi.org/10.1103/PhysRevB.79.045208)

PACS number(s): 71.35.-y, 42.65.Re

I. INTRODUCTION

The generation of ultrafast currents in bulk and low-dimensional semiconductors via coherence control has been a subject of interest for more than a decade.^{1–22} In one particular embodiment, a two-color light beam containing frequency ω and phase-related second harmonic 2ω with $\hbar\omega < E_g < 2\hbar\omega$ has been predicted^{6,7} and observed to induce pure electrical currents,^{8,9} spin-polarized electrical currents,¹⁰ and pure spin currents^{11,12} through the quantum interference of one- and two-photon absorption processes connecting valence and conduction bands separated by a fundamental band gap E_g . Various combinations of semiconductor orientation, relative optical phase, and polarizations of the $\omega/2\omega$ beams can define the type, strength, and directionality of the currents. The current injection process can also be understood as the result of the nonlinear optical mixing of three optical fields to give a dc. For example, in the case of electrical current, a Fermi’s golden rule calculation shows that the time derivative of the injected current \vec{J} is given by⁶

$$\frac{d\vec{J}}{dt} = \vec{\eta} \vec{E}^\omega \vec{E}^\omega \vec{E}^{-2\omega} + \text{c.c.}, \quad (1)$$

where $\vec{E}^{\omega,2\omega}$ are the complex optical-field amplitudes, and $\vec{\eta}$ is a frequency-dependent tensor whose symmetry properties are governed by the illuminated material. During and following optical excitation, the currents are expected to evolve according to subpicosecond momentum relaxation and, in the case of electrical currents, space-charge effects. If electrons and holes are injected with excess energy $2\hbar\omega - E_g$, which is large compared to the exciton binding energy E_x , the carrier kinetic energy dominates the Coulomb interaction energy, the relative phase of electron and hole wave functions is negligible, and the electrons and holes can be treated within the independent-particle approximation. In this case,

corresponding to nearly all experiments reported until the present, $\vec{\eta}$ is purely imaginary. For optical fields collinearly polarized along a crystal axis ($\vec{E}^\omega = E^\omega e^{i\phi_\omega \hat{x}}$ and $\vec{E}^{2\omega} = E^{2\omega} e^{i\phi_{2\omega} \hat{x}}$) the injected current obeys

$$\frac{dJ_x}{dt} = 2|\eta_{xxxx}| E^\omega E^\omega E^{-2\omega} \sin(\Delta\phi), \quad (2)$$

where $\Delta\phi = 2\phi_\omega - \phi_{2\omega}$; i.e., the only phase dependence arises from the external beams.

Recently several groups^{17–22} have theoretically considered the influence of Coulomb interactions on two-color coherent control, a situation optimally revealed when optical excitation is nearly resonant with the band gap. For excitation of continuum states with $0 < 2\hbar\omega - E_g \approx E_x$, i.e., excitation of unbound excitons within the region where Coulomb or Sommerfeld enhancement²³ of optical absorption occurs, Bhat and Sipe¹⁹ suggested that the spin or current injection tensors are similarly enhanced and become *complex* with $\Delta\phi \rightarrow \Delta\phi - \delta_c$, where

$$\delta_c(\omega) = \tan^{-1} \sqrt{\frac{E_x}{2\hbar\omega - E_g}} = \arctan \frac{\Re(\eta)}{\Im(\eta)}. \quad (3)$$

For below band-gap photon energies $-E_x < 2\hbar\omega - E_g \leq 0$ where excitation of bound exciton states occurs, even more dramatic departures from the independent-particle approximation of coherently controlled currents have been theoretically suggested. For example, if excitons of different spatial symmetry are simultaneously excited by photons of the appropriate energy, Marti *et al.*^{17,18} and Rumyantsev and Sipe²⁰ predicted the emergence of ultrafast ac spin and charge currents. In the case of single-photon excitation of $1s$ excitons and two-photon excitation of $2p$ excitons by collinearly polarized second-harmonic and fundamental beams, respec-

tively, the subsequent beating of the two polarizations is expected to lead to an ac, wherein

$$\frac{dJ_x}{dt} = 2|\eta_{xxxx}|\sin(\Omega_{1s-2p}t + \Delta\phi - \delta_{E_x})E^\omega E^\omega E^{-2\omega}. \quad (4)$$

Here $\hbar\Omega_{1s-2p}$ corresponds to the energy separation of $1s$ and $2p$ states, δ_{E_x} is a material/exciton phase parameter and relaxation effects are neglected. In this case the optical phase parameter $\Delta\phi$ results in a phase shift of the injected current, but alone it does not determine its peak amplitude.

Here we report experimental investigations of Coulomb or exciton-related effects on coherently controlled electrical currents in semiconductors with optical excitation of electron-hole pairs in the vicinity of the band gap. As in earlier investigations we consider ultrashort pulse excitation, primarily to obtain sufficient strong two-photon absorption and to operate in a time regime comparable to the momentum scattering time. Several material and optical parameters prescribe the optimum materials for the investigation of Coulomb effects. The fact that current injection efficiency is predicted to sharply decrease with increasing band gap⁹ suggests the use of materials with $E_g < 2.5$ eV. For efficient generation of optical pulses via a Ti:sapphire-pumped optical parametric source, one typically is limited to $0.7 < \hbar\omega < 1$ eV. In addition, E_x should ideally be comparable to—but not much smaller than—the typical bandwidth of the excitation pulses (~ 20 meV for a 150 fs pulse) in order to be able to selectively address pure continuum, Coulomb modified continuum (unbound excitons), or bound exciton states.

In order to achieve a reasonable compromise of the above requirements, we have carried out coherence control experiments in bulk, wurtzite, CdSe ($E_g = 1.82$ and 1.84 eV at²⁴ 80 K for A and B gaps along the c axis), and zinc-blende CdTe ($E_g = 1.606$ eV at²⁵ 1.6 K), using 150 fs fundamental and second-harmonic pulses with $2\hbar\omega \approx E_g$. For CdSe $E_x = 15$ and 16 meV for the A and B gaps,²⁶ respectively. For CdTe,²⁵ $E_x = 10.5$ meV. For the large E_x in these two materials, as compared to, e.g., GaAs and InP, one can more easily distinguish exciton and continuum effects. The electrical currents are characterized through the terahertz emission associated with ultrafast charge displacement with the far-field terahertz field strength proportional to the time derivative of the source current (dJ/dt).²⁷ We have also excited electrical currents in the lower band-gap material InP ($E_g = 1.42$ eV at²⁸ $T = 10$ K with $E_x = 5$ meV).

For InP, with $2\hbar\omega - E_g \gg E_x$ current injection can be considered to occur within the independent-particle approximation so that InP can effectively be used as a reference material. Indeed, relative to InP and for our pulse parameters, we identify pronounced exciton influences on the current generation dynamics in both CdTe and CdSe. For excitation of bound exciton states, we find terahertz emission occurs for every relative phase of the $\omega/2\omega$ excitation field. This finding contradicts the independent-particle picture embodied in Eqs. (1) and (2), but, as seen below, is consistent with the optical generation of the ultrafast ac due to a simultaneous excitation of different exciton states.^{18,20} Upon exciting CdTe at the fundamental band-gap energy, we observe an absolute

phase shift in the terahertz emission pattern, possibly related to the intrinsic phase shift predicted by Bhat and Sipe,¹⁹ however, the interpretation is complicated by the presence of the exciton ac source term. Overall, these results provide insight into the influence of Coulomb interactions on current injection and the influence of many-body effect on resonant optical nonlinearities of semiconductors. Our work can also be seen as complementing recent experimental reports²⁹ in which terahertz absorption rather than emission was used to probe $1s-2p$ exciton states and carrier many-body effects in GaAs and Cu₂O.

II. EXPERIMENTAL

The experimental setup used to observe terahertz emission from coherently controlled currents has been described in detail elsewhere.³⁰ Briefly, a commercial 250 kHz Ti:sapphire amplifier operating at 810 nm is used to pump an optical parametric amplifier to produce 150 fs pulses tunable between 1300 and 1600 nm (0.78 eV $\leq \hbar\omega \leq 0.95$ eV) with an average power of ~ 25 mW. Second-harmonic radiation with ~ 0.5 mW average power is obtained from a 1.5-mm-thick beta barium borate (BBO) crystal. The $\omega/2\omega$ pulses are passed through a two-color Michelson interferometer that allows the relative phase $\Delta\phi$ to be adjusted using piezocontrol. Any slow drift of $\Delta\phi$ is monitored through analysis of spectral interference of either a back reflection of the 2ω beam or a copropagating continuum generated by remnant 810 nm pump light in a sapphire plate. With this monitoring scheme one can produce a stable relative optical phase, although its absolute value is not obtained. The emerging two pump beams are copolarized and overlapped on the samples with a 100 μm diameter full width at half maximum (FWHM) spot size. No care has been taken to fix the polarization relative to the crystal axis, since for the chosen beam polarizations, the dependence is weak. The samples are mounted in a cryostat operated at a temperature of 10 or 80 K. Measurement of the in-plane current dynamics is achieved by electro-optic (EO) sampling of the terahertz radiation emitted in a reflection geometry. Note that sapphire windows in the cryostat, although slightly birefringent, permit good transmission of both near-infrared excitation light and the terahertz emission. Terahertz radiation is detected using electro-optic sampling techniques employing 810 nm (1.53 eV), 150 fs probe pulse from the Ti:sapphire amplifier, and a 500- μm -thick (110)-oriented ZnTe crystal. With $f/2$ parabolic mirror terahertz collection and steering optics, the overall terahertz detection system has a peak response³¹ near a frequency of $\Omega_d/2\pi = 1.5$ THz with a complete bandwidth of $\Delta\Omega_d/2\pi \sim 3$ THz.

III. RESULTS

Experiments were conducted on CdSe at 80 K with $1.75 < 2\hbar\omega < 1.91$ eV and on CdTe at 10 K with $1.58 < 2\hbar\omega < 1.66$ eV. For each of these photon energies, coherence control experiments were also performed using a [100] InP wafer at 10 or 80 K. We first consider the experiments performed on InP. For $2\hbar\omega = 1.82$ eV the single-³² and two-photon^{33,34} absorption coefficients are 3×10^4 cm⁻¹ and

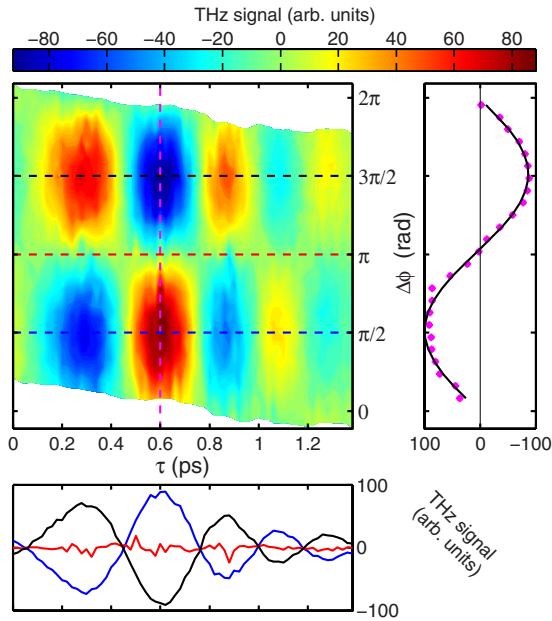


FIG. 1. (Color online) $\Delta\phi$ - τ contour plot of the terahertz radiation field from a [100]-oriented InP wafer at $T=10$ K for 0.8 eV/1.6 eV $\omega/2\omega$ pump and 1.53 eV probe pulse. Optical excitation conditions are given in text. The side panel shows a one-dimensional (1D) plot of the terahertz signal as a function of $\Delta\phi$ for a particular constant value of τ (corresponding to the vertical dashed line in the contour plot), while the bottom panel shows a 1D plot of the terahertz signal as a function of τ for $\Delta\phi=\pi/2$, π , or $3\pi/2$ (corresponding to the horizontal dashed line in the contour plot).

30 cm/GW, respectively. For a peak-focused intensity of $I_\omega=8.5$ GW/cm² ($I_{2\omega}=170$ MW/cm²), a peak carrier density of $N_\omega=1\times 10^{18}$ cm⁻³ ($N_{2\omega}=3\times 10^{18}$ cm⁻³) is obtained. Since $2\hbar\omega-E_g\approx 10E_x$ the currents are generated within the approximations of the independent-particle picture and serve as useful references for the following discussion of the influence of electron-hole interaction effects on currents in CdSe and CdTe. Note that for these carrier densities, the current decay time is likely to be comparable or less than the optical pulse widths due to carrier-carrier- and carrier-phonon-induced momentum relaxation and hence the current temporal profiles should be similar to the optical pulse profiles.

Figure 1 shows a contour plot of the terahertz radiation field from the InP at 10 K as a function of $\Delta\phi$ and the time delay τ between the $\omega/2\omega$ pump and 1.53 eV probe pulses. The data are corrected for a small drift of $\Delta\phi$ as verified from the phase reference within the two-color Michelson interferometer. The $\Delta\phi$ values are not absolute since they can only be determined to within a constant offset as stated above. Similarly no attempt has been made to obtain an absolute value of τ since this is not necessary for our purposes; however, for consistency we define the delay time to be 0.6 ps at the occurrence of the maximum terahertz signal.

Because we take the EO-detected terahertz field profile as a signature of the coherently controlled currents, we must consider to what extent the EO signal provides information about the current. From Eq. (2) one expects the transient charge current injection to have an amplitude $dJ/dt \propto \sin(\Delta\phi)$. For our pulses and materials, if we take into ac-

count the subpicosecond optical excitation and momentum relaxation time, the coherently controlled current would give rise to a far-field terahertz emission spectrum centered at 2 THz with bandwidth (FWHM) of ~ 5 THz. However, since our EO detection system has a peak response at $\Omega_d/2\pi = 1.5$ THz with a bandwidth $\Delta\Omega_d/2\pi < 5$ THz, it effectively filters the incoming radiation to produce a τ -dependent transient signal that is essentially the Fourier transform of the EO system frequency response. Combining the approximately Gaussian spectral response of the EO detector with the phase-dependent amplitude of the current injection, one can easily show³¹ that the detected terahertz field is of the form $E_{\text{THz}}^{\text{det}} \propto \sin(\Delta\phi)\sin(\Omega_d\tau)f(\Delta\Omega_d\tau)$; the $\sin(\Omega_d\tau)$ dependence arises from the dominant frequency response of the detector while $f(\Delta\Omega_d\tau)$ is an envelope function that decays with increasing τ with a characteristic time $\propto \pi/\Delta\Omega_d$ (i.e., ~ 1 ps). Continuum current injection produces a terahertz $\Delta\phi$ - τ contour plot which can be factored in terms of its $\Delta\phi$ and τ dependence to produce a “grid” pattern as shown in Fig. 1. The bottom panel of Fig. 1 shows τ -dependent cuts through the contour for $\Delta\phi=\pi/2$, π , and $3\pi/2$. For $\Delta\phi=\pi/2$ or $3\pi/2$ one observes the decaying sinusoidal, or $\sin(\Omega_d\tau)f(\Delta\Omega_d\tau)$, dependence as expected; for $\Delta\phi=\pi$, to within experimental error, no signal is observed. More importantly for our purposes, as shown in the side panel of Fig. 1, the sign of the terahertz field and thus the direction of the current in the sample reverse as $\Delta\phi$ varies for constant τ and more generally—apart from a possible phase offset—follows a $\sin(\Delta\phi)$ dependence. In particular, the emission strength for $\Delta\phi \approx 0, \pi, 2\pi, \dots$ vanishes to within experimental uncertainty for all delay times. The overall emission pattern observed in Fig. 1 is consistent with the coherent control of photocurrents within the independent-particle picture [cf. Eq. (2)].

We now consider current injection in CdSe. For $2\hbar\omega=1.908$ eV and with single-³² and two-photon³⁵ absorption coefficients of 4.1×10^4 cm⁻¹ and 10 cm/GW, respectively, the same peak-focused intensities as were used for InP are estimated to produce peak carrier density of $N_\omega=3\times 10^{17}$ cm⁻³ ($N_{2\omega}=3\times 10^{18}$ cm⁻³) in CdSe, i.e., nearly the same as in InP. Note that these values of carrier density are approximations when $2\hbar\omega \geq E_g$, where both one- and two-photon absorption coefficients exhibit strong dispersion. Figure 2 displays contour plots of the terahertz radiation field from a (0001)-oriented intrinsic CdSe wafer as a function of $\Delta\phi$ and delay time τ between $\omega/2\omega$ pump and 1.53 eV probe pulses for three different values of $2\hbar\omega$. For $2\hbar\omega=1.908$ eV the emission pattern depicted in Fig. 2(a) has characteristics similar to those seen in Fig. 1. This is not unexpected since $2\hbar\omega-E_g \approx 5E_x$ and the independent-particle picture should be valid. In contrast, for the data in Fig. 2(c), $2\hbar\omega=1.826$ eV ~ 0 and one can excite bound excitons within the bandwidth of the laser pulses. Most strikingly, terahertz emission is observed for every choice of $\Delta\phi$ inconsistent with Eq. (1). [Note that the phase drift correction is largest for Fig. 2(c); this is related to the lower signal levels which required longer scan times and hence yield larger phase drift.] For an intermediate photon energy of $2\hbar\omega=1.85$ eV, $2\hbar\omega-E_g \approx E_x$ and Fig. 2(b) shows results intermediate between that of Figs. 2(a) and 2(c). Note that

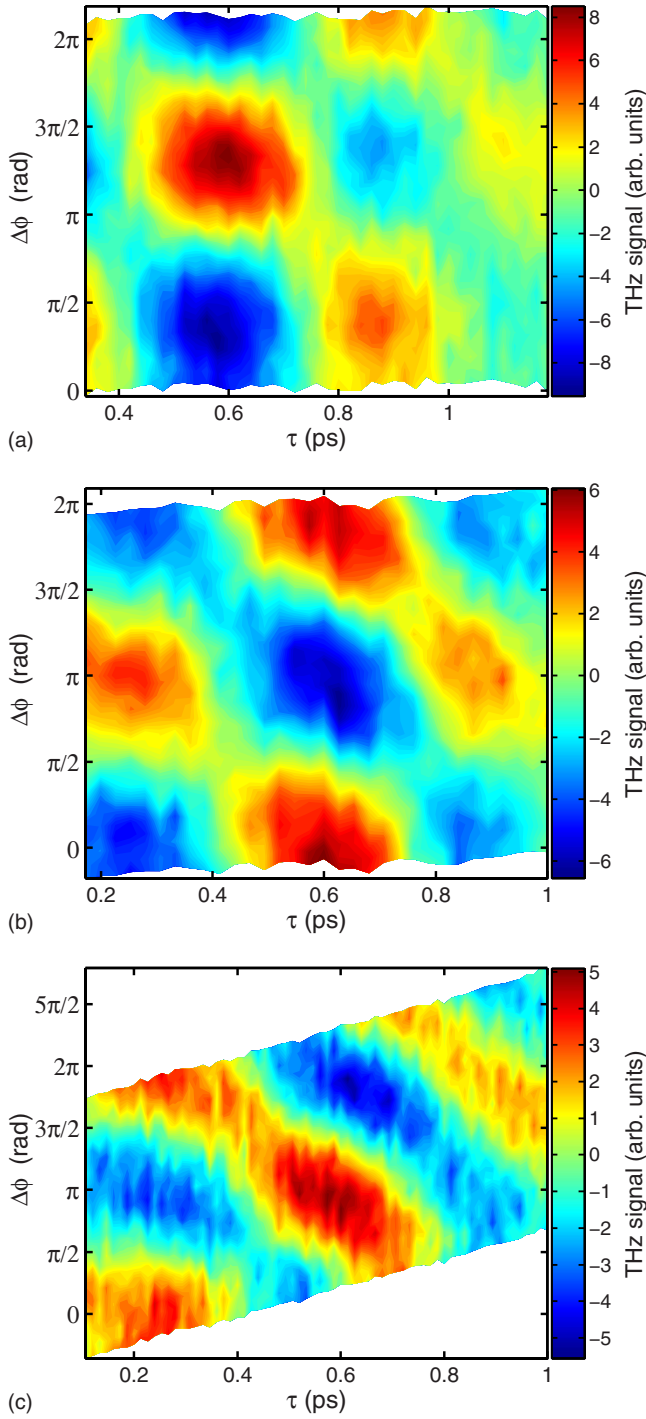


FIG. 2. (Color online) $\Delta\phi$ - τ contour plots of terahertz radiation field from a (0001) CdSe wafer at $T=80$ K for $2\hbar\omega=(a)$ 1.908 eV, (b) 1.850 eV, and (c) 1.826 eV. Note that the value of $\Delta\phi$ likely has an offset between the three panels; the skew in the figures [most apparent in (c)] is related to corrections to the raw data to account for a phase drift.

given the pulse bandwidths, for this particular photon energy one can still excite excitons. We have also observed the terahertz emission from CdSe for a temperature of 10 K (data not shown here). Apart from wavelength shifts associated with the change in the band-gap energy, the terahertz emission patterns are very similar at $T=10$ and 80 K.

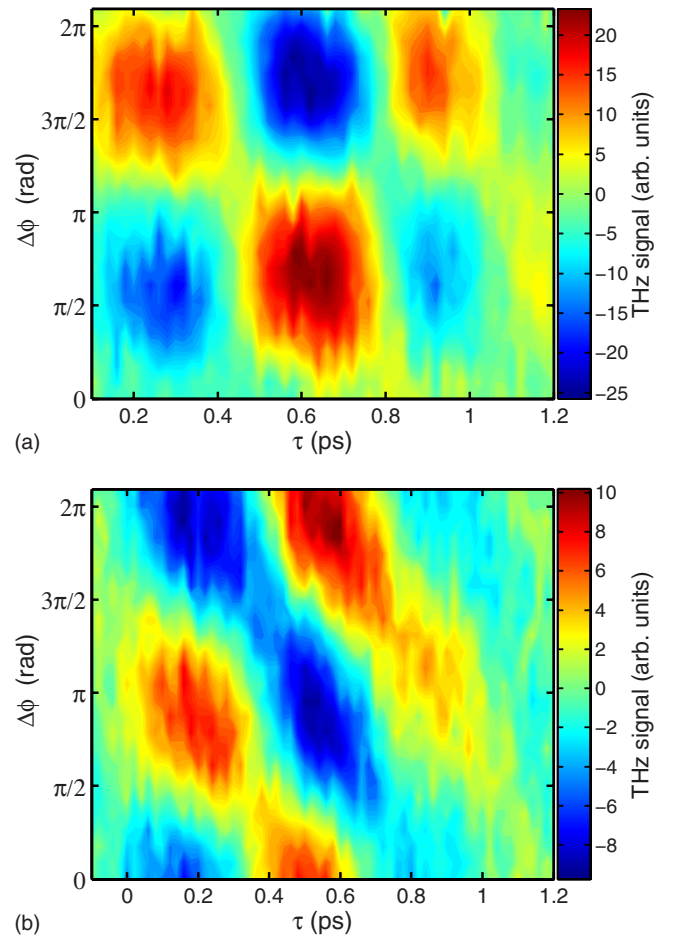


FIG. 3. (Color online) $\Delta\phi$ - τ contour plot of terahertz radiation field from a [100] oriented CdTe wafer at $T=10$ K for $2\hbar\omega=(a)$ 1.653 eV and (b) 1.610 eV. Note that the value of $\Delta\phi$ likely has an offset between panels.

Since it might be argued that the results displayed in Fig. 2 may in part be related to the complex bandstructure of the wurtzite CdSe, we have carried out related current injection experiments in zinc-blende CdTe. With $2\hbar\omega=1.653$ eV, for which the single-³² and two-photon³⁴ absorption coefficients are 2×10^4 cm^{-1} and 20 cm/GW , respectively, a peak carrier density of $N_\omega=1 \times 10^{18}$ cm^{-3} ($N_{2\omega}=2 \times 10^{18}$ cm^{-3}) is obtained for peak-focused intensities similar to that used with InP and CdSe. Figure 3 shows the terahertz emission contour plots for $2\hbar\omega=1.65$ and 1.61 eV. Most interestingly, the emission patterns largely resemble the experimental trends seen in CdSe. In particular, for Fig. 3(a) where $2\hbar\omega-E_g \approx 5E_x$ the terahertz emission $\Delta\phi$ - τ contour plot is essentially consistent with the independent-particle picture represented by Eq. (2) and the experimental results of Fig. 2(a). In contrast, for Fig. 3(b) where $2\hbar\omega-E_g \approx 0$, there is a distortion of the emission pattern similar to that observed in Fig. 2(b). It might be noted that we observe no terahertz signal when one of the pump beams is removed. This eliminates the possibility that any part of our terahertz signal may be related to effects induced by a single color beam. Note that the excitation conditions in Fig. 3(b) also result in the generation of electron-hole pairs in the Sommerfeld en-

hanced continuum close to the fundamental band gap.

IV. DISCUSSION

The CdSe and CdTe data give strong evidence for deviations from the independent-particle picture of coherently controlled electrical currents in semiconductors as one tunes $2\hbar\omega$ in the vicinity of their band gap. Since similar deviations are not observed in InP at any of the photon energies used, we can exclude experimental artifacts. However, besides effects related to the EO detection response as discussed above, we should also consider how the linear optical properties, space-charge fields, and momentum relaxation, change with tuning of the pump frequencies. We discuss these in turn.

In the case of the polarization ac for CdSe (CdTe) $\Omega_{1s-2p}/2\pi=3.5$ THz (2.5 THz). The peak frequency of terahertz emission for ac excitation is therefore higher than the frequency $\Omega_d/2\pi$ associated with the peak response of the EO sampling detection system. When the EO system response is taken into account, for a current source given by Eq. (4), for an analysis similar to that used for InP above we find that $E_{\text{THz}}^{\text{det}} \propto \sin(\Omega_d\tau + \Delta\phi - \delta_{Ex})f(\Delta\Omega_d\tau)$. That is, the phase parameter $\Delta\phi$ produces a phase shift of the current and detected terahertz radiation but does not alone control their amplitude as it does for continuum-based currents. Both continuum and exciton-detected signals have frequency and decay characteristics dictated by the EO detection system but with a very different $\Delta\phi$ dependence. Dividing out the common terahertz envelope/decay time effect, one can easily show that the total continuum and exciton-detected terahertz signal produced by the EO sampling technique effectively varies with pump-probe delay τ as

$$E_{\text{THz}}^{\text{det}} \propto A(\omega)\sin(\Delta\phi - \delta_c)\sin(\Omega_d\tau) + B(\omega)\sin(\Omega_d\tau + \Delta\phi - \delta_{Ex}). \quad (5)$$

Here, the first term of amplitude $A(\omega)$ relates to continuum “dc” source, while the second term of amplitude $B(\omega)$ relates to the $1s-2p$ exciton ac source current. For $2\hbar\omega - E_g \gg E_x$ (or equivalently \gg the pump pulse energy bandwidth) one expects the first (continuum) term in Eq. (5) to dominate with $\delta_c=0$. This produces the characteristic grid pattern observed in Fig. 1 for InP and in Fig. 2(a) for CdSe and Fig. 3(a) for CdTe. However, when $2\hbar\omega$ decreases toward the band-gap energy, one might expect to see a photon energy-dependent phase shift related to the continuum source. In addition as the pulse bandwidths allow for terahertz emission from a $1s-2p$ exciton ac [second term of Eq. (5)], a $\Delta\phi-\tau$ contour plot should show constant amplitude when $\Omega_d\tau + \Delta\phi$ is constant. This appears as a “diagonal” contribution, in addition to the “grid” contribution, in a $\Delta\phi-\tau$ contour plots as is—in fact—observed in Figs. 2(b), 2(c), and 3(b). By fitting Eq. (4) to the data in the $\Delta\phi-\tau$ contour plots, we can determine the ratio of exciton ac and continuum “dc” contributions $B(\omega)/A(\omega)$.

Figure 4 summarizes the experimental values of $B(\omega)/A(\omega)$ for both CdSe and CdTe for several values of $2\hbar\omega$. The vertical spread in the data reflects experimental uncertainties and limitations associated with extracting am-

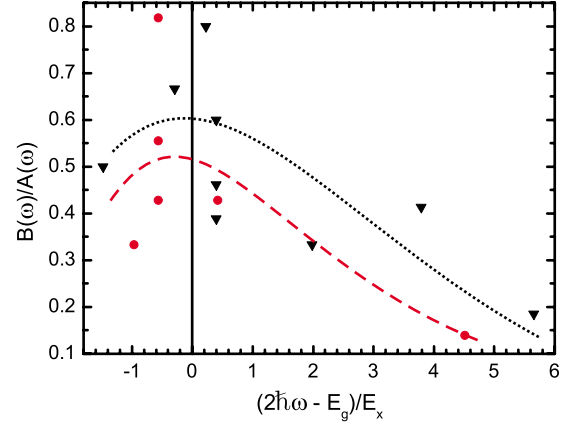


FIG. 4. (Color online) Ratio of the exciton and continuum amplitudes to the EO signal in the terahertz $\Delta\phi-\tau$ contour plots for CdSe (inverted triangles: $T=80$ K) and CdTe (circles: $T=10$ K) as a function of the ratio of injected carrier kinetic energy to exciton energy. The dashed curves are guides for the eyes based on Gaussian curves.

plitudes from periodic signal for the limited number of cycles for which one can maintain reasonable phase stability. For both materials and all the temperatures of this study, we find $B(\omega)/A(\omega)$ to be a maximum for $2\hbar\omega \approx E_g$ and decreasing for larger or smaller photon energies. Note however that the ratio differs from zero for values of $|2\hbar\omega - E_g|/E_x$ much larger than unity. This can be explained in terms of the spectral bandwidth of the pulses. As noted in Sec. I, the current or terahertz generation can be viewed as a nonlinear mixing of frequencies extracted from two fundamental and one second-harmonic pulse. The available optical bandwidth is therefore the bandwidth of the spectral convolution of the *fields* of these three pulses. Assuming that each of these pulses has an *intensity* FWHM bandwidth of 20 meV, the bandwidth of the convolved pulses, assuming Gaussian temporal profile, has a bandwidth of $2^{3/2}(20 \text{ meV}) \sim 60 \text{ meV}$. In addition, broadening can be expected from the excitons themselves, e.g., due to the density of carriers generated. The width of the spectral response seen in Fig. 4 is on the order of 80 meV, in reasonable agreement with these bandwidth/broadening considerations.

We now consider whether the energy-dependent continuum phase shift $\delta_c(\omega)$ is apparent in the terahertz emission data. At a first glance, this modification should be observable as a simple vertical shift of the emission patterns in the $\Delta\phi-\tau$ plot. To verify this aspect, we have compared the $\Delta\phi$ dependence of the terahertz signal with respect to the reference sample InP when only excitation pulses mainly excite the continuum. As noted previously, any slow phase drift is monitored constantly so that we can extract meaningful phase changes between different samples. We have therefore measured the $\Delta\phi - \delta_c(\omega)$ value corresponding to the maximum terahertz field strength in CdTe relative to the maximum observed in InP, i.e., at $\Delta\phi = \pi/2$. Subtracting this value from the extracted CdTe-InP relative phase shift gives us the δ_c phase shift shown in Fig. 5. Also shown is the theoretical prediction of $\delta_c(\omega)$ from Bhat and Sipe²⁰ as given by Eq. (3). The theoretical and dispersive behavior appears

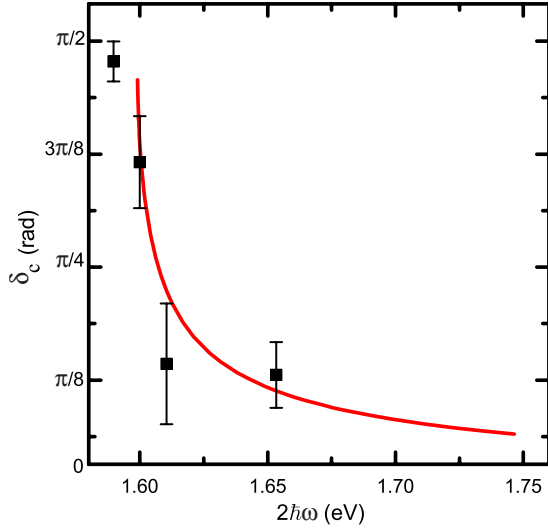


FIG. 5. (Color online) Material phase shift δ_c as a function of photon energy extracted from the $\Delta\phi$ - τ terahertz contour plots for CdTe at $T=10$ K. The solid curve is based on the theoretical prediction by Bhat and Sipe (Ref. 19) [Eq. (3)] shifted vertically by 0.5 rad to compensate for a material-dependent intrinsic phase related to the linear optical properties.

to be in agreement. In arriving at the data of Fig. 4 we have removed a background 0.5 rad phase shift. There can be several reasons for such a uniform shift, the principal one being that current generation and terahertz emission are spatially distributed along the absorption depth $\alpha_{2\omega}^{-1}$ of the optical pulses. Within this depth, due to the different refractive indices at ω and the 2ω , there can be a phase walkoff of the two pump beams. Indeed, one can easily show that the optical phase walkoff leads to a phase shift in the current generation process of $\delta_{\text{dis}} = \tan^{-1}[4\omega c^{-1}\alpha_{2\omega}^{-1}(n_{2\omega} - n_\omega)]$. Using values of the linear optical constants,³² we find $\delta_{\text{dis}} \sim 0.4$ rad for CdTe for the full range of photon energies used

in the experiments. However, we note that a superposition of pure continuum and bound exciton currents with different relative phase could yield a similar dependence of the terahertz phase on photon energy; the signal to noise in the present experiment does not allow for the use of narrow-band excitation pulses to achieve a more specific excitation to separate out continuum and excitonic effects for excitation near the band edge. We have also tried to identify similar absolute phase changes in the emission patterns of CdSe. In this case, we are not able to resolve an intrinsic phase δ_c , not surprising in view of the more complex behavior of a wurtzite semiconductor with A - and B -exciton transitions.

V. SUMMARY

In conclusion, we have carried out detailed studies of two-color coherent injection of electrical currents in CdSe and CdTe using excitation in the vicinity of the band edge and using terahertz emission signatures to observe the currents. Our results show clear indication of a departure from the independent-particle picture of electron-hole injection. The dependence of terahertz emission on relative phase of the pump beams and time delay indicates the appearance of a contribution that is consistent with the excitation of an ac exciton polarization current. In addition there is possible evidence of a phase shift of the continuum dc contribution related to electron-hole interactions, although the evidence is complicated by the presence of the exciton contribution, due to the bandwidth of the excitation pulses.

ACKNOWLEDGMENTS

We thank John Sipe for helpful discussions. We are grateful to NSERC and the Office of Naval Research for financial support. J.-M.M. acknowledges support from the Walter C. Sumner Foundation while M.B. is thankful for support from the Alexander von Humboldt Foundation.

*Corresponding author; vandriel@physics.utoronto.ca

¹E. M. Baskin and M. V. Éntin, JETP Lett. **48**, 601 (1988).

²M. V. Éntin, Sov. Phys. Semicond. **23**, 664 (1989).

³G. Kurizki, M. Shapiro, and P. Brumer, Phys. Rev. B **39**, 3435 (1989).

⁴B. I. Sturman and V. M. Fridkin, *The Photovoltaic and Photo-refractive Effects in Noncentrosymmetric Materials* (Gordon and Breach, Philadelphia, 1992).

⁵E. Dupont, P. B. Corkum, H. C. Liu, M. Buchanan, and Z. R. Wasilewski, Phys. Rev. Lett. **74**, 3596 (1995).

⁶R. Atanasov, A. Haché, J. L. P. Hughes, H. M. van Driel, and J. E. Sipe, Phys. Rev. Lett. **76**, 1703 (1996).

⁷R. D. R. Bhat and J. E. Sipe, Phys. Rev. Lett. **85**, 5432 (2000).

⁸A. Haché, Y. Kostoulas, R. Atanasov, J. L. P. Hughes, J. E. Sipe, and H. M. van Driel, Phys. Rev. Lett. **78**, 306 (1997).

⁹M. Sheik-Bahae, Phys. Rev. B **60**, R11257 (1999).

¹⁰M. J. Stevens, A. L. Smirl, R. D. R. Bhat, J. E. Sipe, and H. M. van Driel, J. Appl. Phys. **91**, 4382 (2002).

¹¹M. J. Stevens, A. L. Smirl, R. D. R. Bhat, A. Najmaie, J. E. Sipe, and H. M. van Driel, Phys. Rev. Lett. **90**, 136603 (2003).

¹²J. Hübner, W. W. Rühle, M. Klude, D. Hommel, R. D. R. Bhat, J. E. Sipe, and H. M. van Driel, Phys. Rev. Lett. **90**, 216601 (2003).

¹³S. D. Ganichev, E. L. Ivchenko, V. V. Bel'kov, S. A. Tarasenko, M. Sollinger, D. Weiss, W. Wegscheider, and W. Prettl, Nature (London) **417**, 153 (2002).

¹⁴T. M. Fortier, P. A. Roos, D. J. Jones, S. T. Cundiff, R. D. R. Bhat, and J. E. Sipe, Phys. Rev. Lett. **92**, 147403 (2004).

¹⁵M. Bieler, K. Pierz, U. Siegner, and P. Dawson, Phys. Rev. B **73**, 241312(R) (2006).

¹⁶L. Costa, M. Betz, M. Spasenović, A. D. Bristow, and H. M. van Driel, Nat. Phys. **3**, 632 (2007).

¹⁷D. H. Marti, M.-A. Dupertuis, and B. Deveaud, Phys. Rev. B **69**, 035335 (2004).

¹⁸D. H. Marti, M.-A. Dupertuis, and B. Deveaud, Phys. Rev. B **72**, 075357 (2005).

- ¹⁹R. D. R. Bhat and J. E. Sipe, Phys. Rev. B **72**, 075205 (2005).
- ²⁰I. Romyantsev and J. E. Sipe, Phys. Rev. B **73**, 201302(R) (2006).
- ²¹H. T. Duc, T. Meier, and S. W. Koch, Phys. Rev. Lett. **95**, 086606 (2005).
- ²²H. T. Duc, Q. T. Vu, T. Meier, H. Haug, and S. W. Koch, Phys. Rev. B **74**, 165328 (2006).
- ²³H. Haug and S. W. Koch, *Quantum Theory of the Optical and Electronic Properties of Semiconductors* (World Scientific, Singapore, 1993).
- ²⁴K. A. Dmitrenko, L. V. Taranenko, S. G. Shevell, and A. V. Marinchenko, Sov. Phys. Semicond. **19**, 487 (1985).
- ²⁵S. Adachi, *II-IV Compound Semiconductors*, Handbook of Physical Properties of Semiconductors Vol. 3 (Kluwer Academic, New York, 2004).
- ²⁶J. Voigt, F. Spiegelberg, and M. Senoner, Phys. Status Solidi B **91**, 189 (1979).
- ²⁷D. Côté, N. Laman, and H. M. van Driel, Appl. Phys. Lett. **80**, 905 (2002); D. Côté, J. E. Sipe, and H. M. van Driel, J. Opt. Soc. Am. B **20**, 1374 (2003).
- ²⁸*Semiconductors—Basic Data*, 2nd ed., edited by O. Madelung (Springer-Verlag, Berlin, 1996).
- ²⁹R. Huber, B. A. Schmidt, R. A. Kaindl, and D. S. Chemla, Phys. Status Solidi B **245**, 1041 (2008).
- ³⁰M. Spasenović, M. Betz, L. Costa, and H. M. van Driel, Phys. Rev. B **77**, 085201 (2008).
- ³¹G. Gallot and D. Grischkowsky, J. Opt. Soc. Am. B **16**, 1204 (1999).
- ³²E. D. Palik, *Handbook of Optical Constants of Solids*, 2nd ed. (Academic, New York, 1985).
- ³³D. Vignaud, J. F. Lampin, and F. Mallot, Appl. Phys. Lett. **85**, 239 (2004).
- ³⁴E. W. VanStryland, M. A. Woodall, H. Vanhersele, and M. J. Soileau, Opt. Lett. **10**, 490 (1985).
- ³⁵I. B. Zotova and Y. J. Ding, Appl. Opt. **40**, 6654 (2001).